

Global event properties in proton-proton physics with ALICE

A. Giovannini and R. Ugoccioni

Dipartimento di Fisica Teorica and I.N.F.N. – sezione di Torino
via P. Giuria 1, 10125 Torino, Italy

Abstract

ALICE is a unique opportunity for studying low p_t physics and minimum bias events, and consequently for hunting substructures in strong interactions. The general question concerning global event properties in pp and $p\bar{p}$ physics is indeed whether substructures can be seen in the data in a model-independent way. In other terms, can we identify the interface between perturbative and non-perturbative regimes?

Contribution to the ALICE Physics Performance Report, to appear.

1 Introduction

ALICE is a unique opportunity for studying low p_t physics and minimum bias events, and consequently for hunting substructures in strong interactions. The general question concerning global event properties in pp and p \bar{p} physics is indeed whether substructures can be seen in the data in a model-independent way. In other terms, can we identify the interface between perturbative and non-perturbative regimes?

A successful approach to this question has recently emerged [1], as will be shown in the following.

2 A summary of substructure hunt in pp collisions

What is known on the subject comes from data taken at ISR, at Sp \bar{p} S collider (UA1, UA2 and UA5 experiments) and the Tevatron collider (CDF and E735 experiments) as well as from dedicated theoretical work.

2.1 Energy widening of multiplicity distributions.

It is to be stressed that recent results from Tevatron (E735 Collaboration, [2]) on full phase space multiplicity distributions do not completely agree with those obtained at comparable energies at the Sp \bar{p} S collider (UA5 Collaboration, [3, 4]), see Fig. 1. Tevatron data are more precise than Sp \bar{p} S data at larger multiplicities (they have larger statistics and extend to larger multiplicities than UA5 data), but much less precise at low multiplicity. Both sets of data show a shoulder structure, but the Tevatron MD is somewhat wider. It should be noticed that E735 data are measured only in $|\eta| < 3.25$ and $p_t > 0.2$ GeV/c then extended to full phase space via a Monte Carlo program.

A standing problem!

2.2 The fit with two negative binomial distributions.

The negative binomial (NB) behaviour for final charged particles multiplicity distributions can be trusted in hadron-hadron collisions in full phase space only up to ISR energies [5]. At higher energies shoulder structures start to be clearly visible as shown by the UA5 Collaboration at CERN p \bar{p} collider [4]. The idea firstly suggested by C. Fuglesang [6] is to explain observed NB regularity violations as the effect of the weighted superposition of two classes of events, the multiplicity distribution of each component being of NB type:

$$P_n(\alpha_{\text{soft}}; \bar{n}_{\text{soft}}, k_{\text{soft}}; \bar{n}_{\text{semi-hard}}, k_{\text{semi-hard}}) = \alpha_{\text{soft}} P_n^{\text{NB}}(\bar{n}_{\text{soft}}, k_{\text{soft}}) + (1 - \alpha_{\text{soft}}) P_n^{\text{NB}}(\bar{n}_{\text{semi-hard}}, k_{\text{semi-hard}}); \quad (1)$$

where, for each class, \bar{n} is the average multiplicity and parameter k is linked to the dispersion D by $k^{-1} = D^2/\langle n \rangle^2 - 1/\langle n \rangle$. The two classes are interpreted as soft events (events without mini-jets) and semi-hard events (events with mini-jets) and consequently the weight α_{soft} is the fraction of events without mini-jets as measured by UA1 [7]. The conclusion is that the proposed fit in terms of the superposition of two negative binomial multiplicity distributions (NBMD's) is quite good.

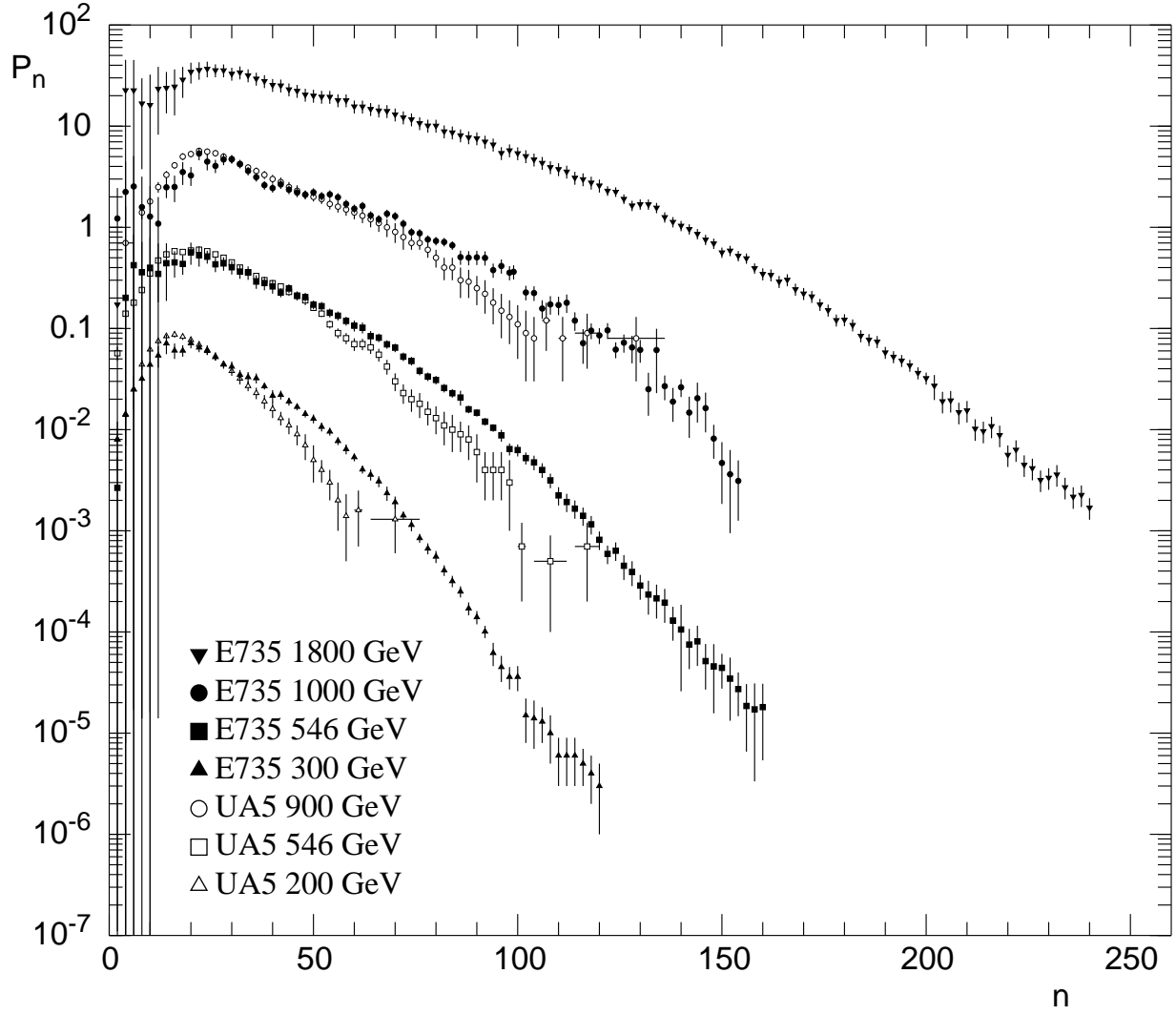


Figure 1: E735 results on charged particle multiplicity distributions in full phase space compared with UA5 results [2]. Data from the two experiments which were taken at nearly the same energy are rescaled by the same factor.

2.3 Extrapolations to LHC energy.

The point is to find acceptable energy dependence of the NB parameters k and \bar{n} for the two components substructures and the corresponding weight factor α_{soft} . In a region where QCD has no predictions one must proceed by phenomenological assumptions [8, 9], which are summarised in the following.

The first assumption concerns energy dependence of the total average charged particle multiplicity [8]:

$$\bar{n} = 3.01 - 0.474 \ln \sqrt{s} + 0.745 \ln^2 \sqrt{s}. \quad (2)$$

The $\ln^2 s$ term is interpreted as the effect of the sharp increase of minijet production and/or double (even triple) parton collisions as suggested by the rapid increase of $\langle p_t \rangle$ with multiplicity. Since below 200 GeV c.m. energy one single NB describes multiplicity distribution data very

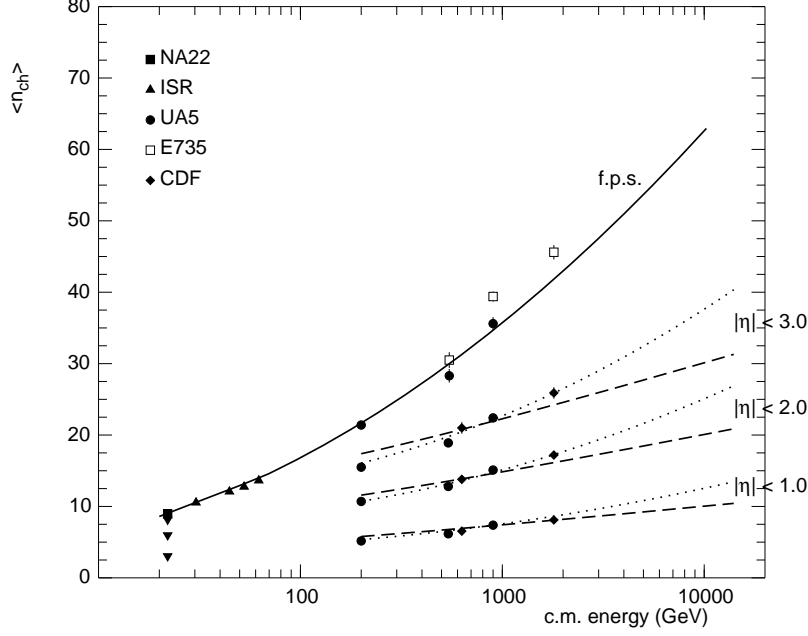


Figure 2: Average charged multiplicity in full phase space and in three pseudo-rapidity interval vs. c.m. energy. Experimental data shown refer to non-single-diffractive data. The solid line shows Eq. (2), the dashed and dotted lines are described in the text.

well and above 200 GeV c.m. energy the soft component has been disentangled, it is proposed to extrapolate the logarithmic increase with energy of the average charged particle multiplicity of the soft component, \bar{n}_{soft} , also at higher c.m. energy. From \bar{n} and \bar{n}_{soft} , one can calculate the behaviour of α_{soft} , which, using the UA1 result $\bar{n}_{\text{semi-hard}} \approx 2\bar{n}_{\text{soft}}$, gives $\alpha_{\text{soft}} \approx 0$ at 100 TeV, but, if one allows again a $\ln^2 s$ term in $\bar{n}_{\text{semi-hard}}$ (with a small coefficient, of the order of 0.1, it is also consistent with the data) one still gets at that energy a sizable (20%) contribution from soft events.

The second assumption concerns the energy dependence of the NB parameter k . For the soft component, KNO scaling was assumed, since it was found to hold in the ISR region. For the semi-hard components three scenarios were examined, two extreme ones (scenario 1 in which the semi-hard component also obeys KNO scaling and scenario 2 in which the semi-hard component violates KNO scaling with $1/k$ growing linearly with $\ln s$) and an intermediate case (scenario 3, where $1/k$ grows not as fast as linearly with a shape inspired by pQCD calculation).

The behaviour of \bar{n} in the TeV region based on UA5 data (Eq. (2)) is shown in Fig. 2 (solid line). It is compared with the mentioned E735 results [2] obtained by extrapolating to full phase space experimental data with a Monte Carlo calculation; observed discrepancies are clearly consequences of the differences noticed between E735 results and UA5 data on charged particle multiplicity distributions shown in Fig. 1 and discussed in Section 2.1. Accordingly, one relies on Eq. (2) predictions.

Coming to particle rapidity density it should be pointed out that by assuming only a longitudinal growth of phase space and constant height of the rapidity plateau with c.m. energy for semi-hard events, as done in Ref. [9], CDF data [10] in pseudorapidity intervals are underestimated (see Fig. 2, dashed lines). These data are well described by allowing a $\ln^2 s$ growth

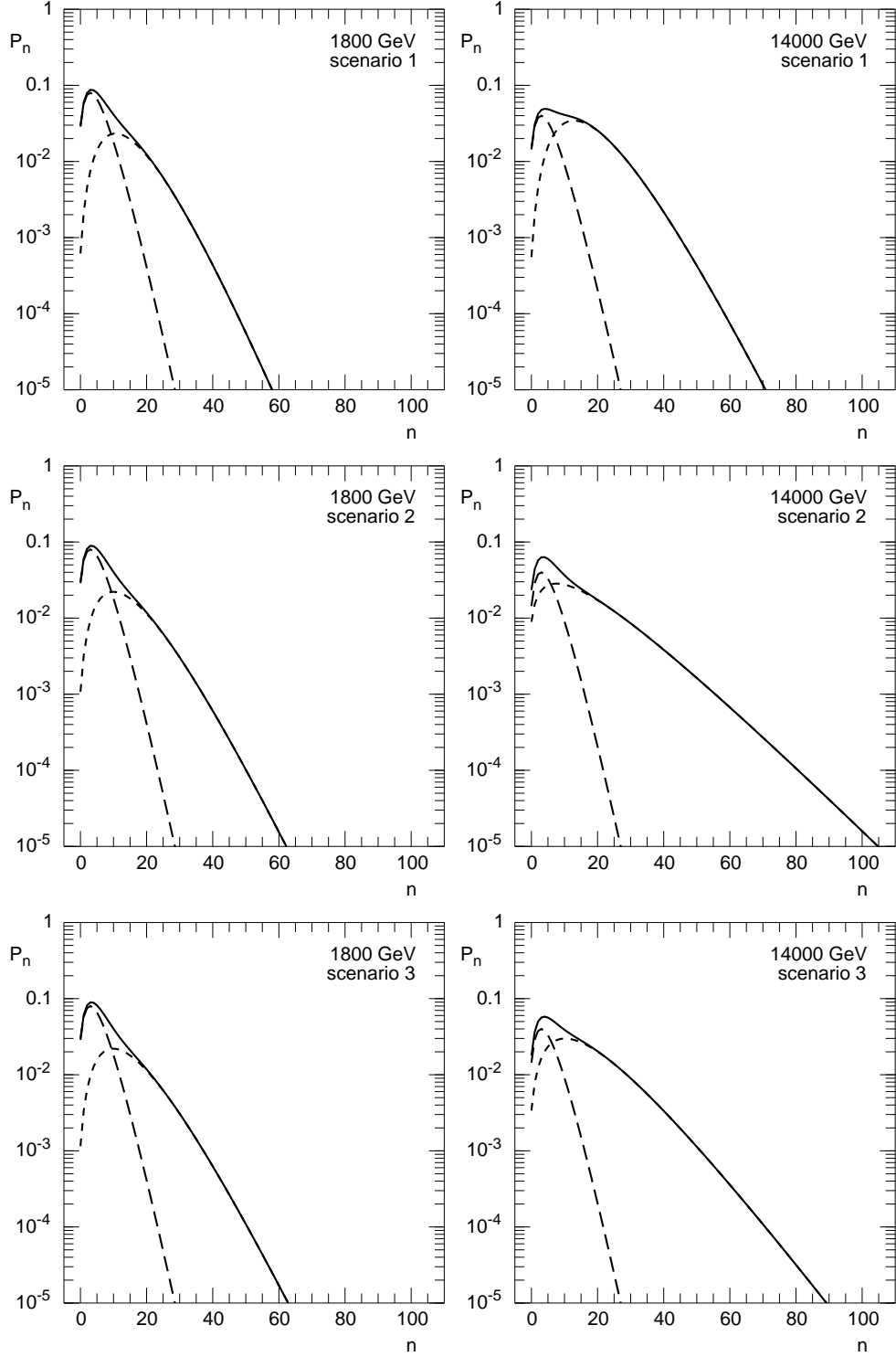


Figure 3: Predicted charged particle multiplicity distributions in the two component model [9] for the interval $|\eta| < 1$ at Tevatron and LHC energies, where the two components (dashed lines) are scaled by α_{soft} and $1 - \alpha_{\text{soft}}$ respectively, Eq. (1), with $\alpha_{\text{soft}} = 0.6$ at 1800 GeV and 0.3 at 14 TeV.

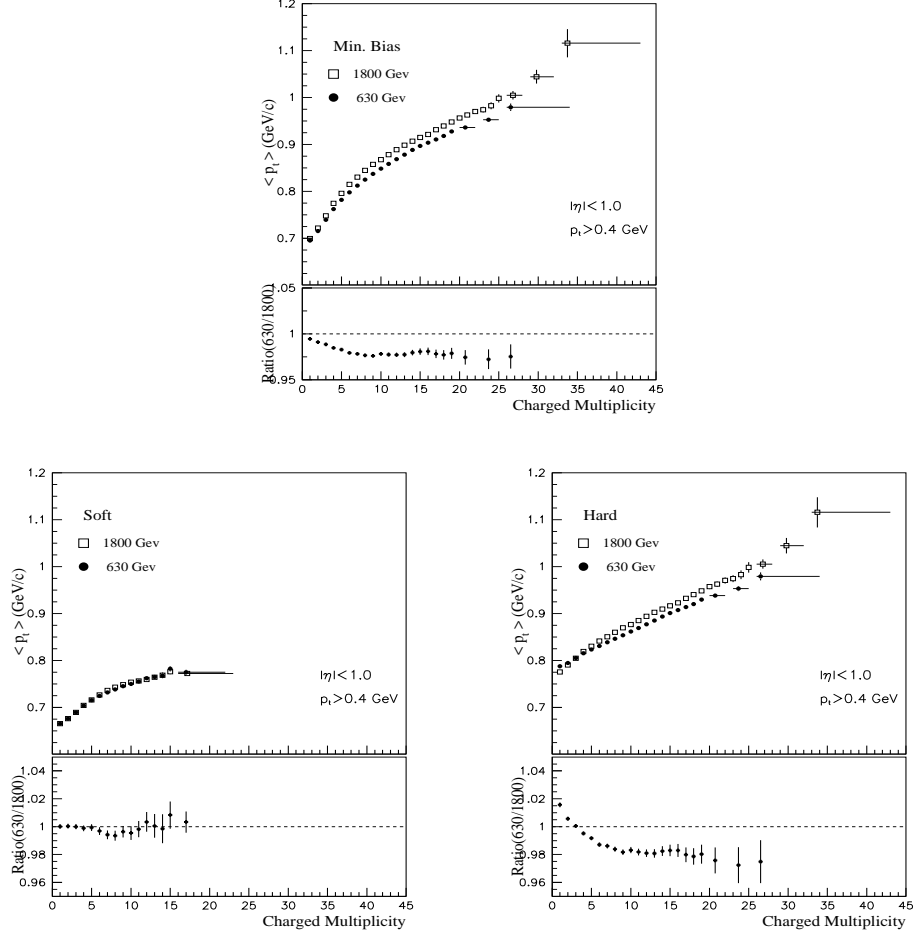


Figure 4: CDF measurements on average transverse momentum vs multiplicity in the full sample and in different classes of events (with and without minijets, called resp. ‘hard’ and ‘soft’ in this figure) [11]

of the total rapidity plateau (Fig. 2, dotted lines): from this consideration one deduces a more appropriate growth of the semi-hard plateau height; the constraint is that $\bar{n}_{\text{semi-hard}}$ in full phase space follows a logarithmic growth with \sqrt{s} as discussed above. Predicted charged particle multiplicity distributions in the three scenarios of the two component model [9] for the interval $|\eta| < 1$ at Tevatron and LHC energies, calculated for the last mentioned case, are shown in Fig. 3 (notice that the comparison with CDF data, in view of the relatively large value of their resolution $p_t > 0.4 \text{ GeV/c}$, is questionable). If this behaviour for the semi-hard component will be confirmed by data one should conclude that semi-hard events populate mainly the central rapidity region giving an important contribution to the increase of charged particle density in central rapidity intervals.

2.4 Soft and hard samples at Tevatron.

It was found by CDF [12] that by subdividing the minimum bias sample into two groups, characterised respectively by the absence (‘soft’ events) or the presence (‘hard’ events) of mini-jets, interesting features of the reaction can be investigated. More precisely, a ‘hard’ event has been

defined as an event with at least one calorimeter cluster in $|\eta| < 2.4$, a cluster being defined as a seed calorimeter tower with at least 1 GeV transverse energy E_t plus at least one contiguous tower with $E_t \geq 0.1$ GeV. A subdivision which is interesting per se and can be tested at 14 TeV.

In summary, the soft component is found to satisfy KNO scaling (as expected in [9]), while the hard one does not; also the $\langle p_t \rangle$ distribution scales at fixed multiplicity in the soft component and not in the hard one; the dispersion of $\langle p_t \rangle$ vs. the inverse of the multiplicity is compatible with an extrapolation to 0 as $n \rightarrow \infty$ in the soft component but not in the hard one, indicating in this limit a lack of correlations in the soft component.

The correlation between $\langle p_t \rangle$ and multiplicity was explained by UA1 [13] as related to the onset of gluon radiation. It should be noticed that at CDF such a correlation is found to some extent for both the soft and the hard subsamples as shown in Fig. 4, but the soft subsample is seen to start to saturate (CDF data shown have $|\eta| < 1.0$ and $p_t > 0.4$ GeV/c).

2.5 Low and high transverse momentum at $Sp\bar{p}S$.

An investigation has been recently carried out [14] on UA1 data also based on the superposition idea: particles are selected according to their p_t (this selection should be contrasted with that performed by CDF in terms of classes of events). It is seen that the high- p_t sample ($p_t > 0.7$ GeV/c) behaves very differently from the low- p_t sample. This difference is interpreted as the effect of a more intense jet-like activity in the high- p_t sample. As far as the low- p_t sample is concerned, it was shown that the dependence of the correlation strength and of higher order cumulants on multiplicity is important in order to test different theoretical models (Monte Carlos are totally inadequate here): for this task the low- p_t cut-off of ALICE at LHC is required. In addition, it would be very interesting to analyse in this way the soft and semi-hard components.

2.6 Average transverse momentum versus multiplicity.

The study should be mentioned at Tevatron (E735) [15] of the correlation between $\langle p_t \rangle$ and multiplicity done separately for pion, kaons and antiprotons, which shows that the behaviour is rather different, as illustrated in Fig. 5, and still not theoretically understood. Data show saturation in p_t at large multiplicity for π^\pm , not for K^\pm and \bar{p} (but for kaons it saturates if a cut is imposed on momenta $p_t < 1.5$ GeV/c, see [16]). At LHC, with 10^9 events, the predictions discussed in Section 2.3 allow the possibility to reach densities from 40 (scenario 1) to 60 (scenario 2) particles per unit rapidity, with good statistics (1000 events). This fact has far reaching consequences which can be tested with ALICE especially at low momentum and the study can be extended to baryon production in the central region (Alice can also measure Λ). All this, plus the relative abundance of particle species, carries precious information on possible quark-gluon plasma formation, in particular in view of such properties as strangeness enhancement and baryon stopping (see elsewhere in this Chapter).

3 Investigations in pp collisions with ALICE

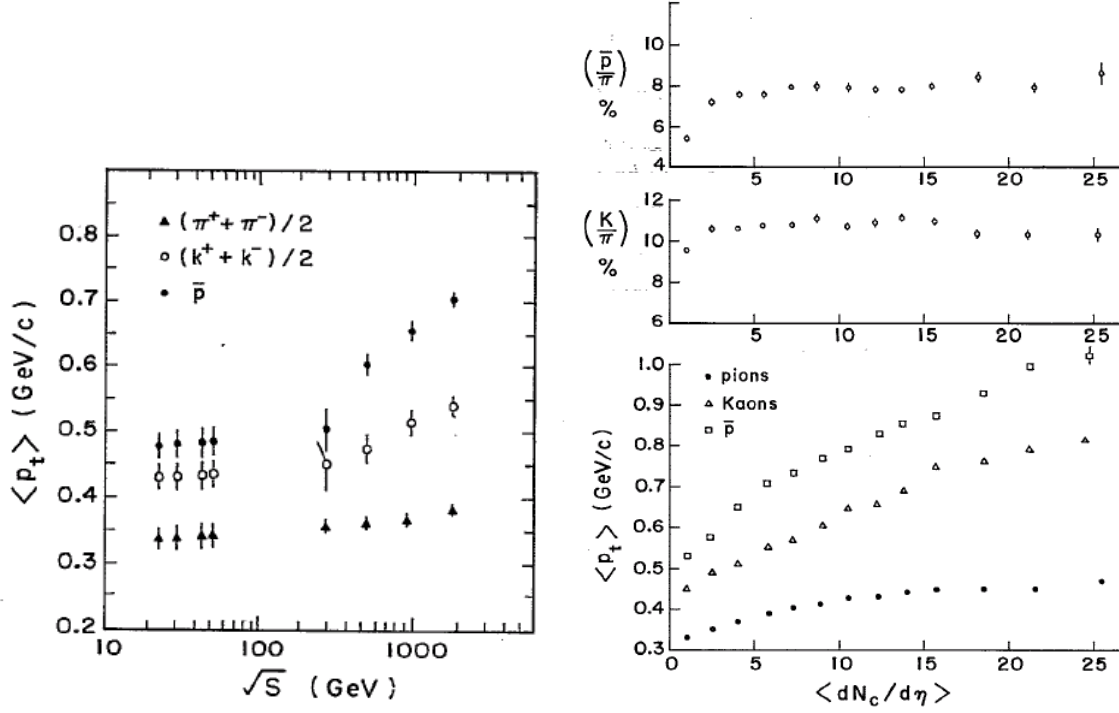


Figure 5: Measurements by E735 [15] of average p_t for identified particles vs. c.m. energy and vs. particle density. The relative abundance of particles is also shown as a function of particle density.

3.1 Shape of the multiplicity distribution.

The average multiplicity $\langle n \rangle$ grows with the c.m. energy \sqrt{s} : the best fit involves a term proportional to $\ln^2 s$, whose theoretical basis is not yet understood. Most theoretical works predict in fact a power-law in s or a linear rise with $\ln s$. Is LHC energy large enough to distinguish these behaviours? Purely statistical extrapolation based on the above mentioned scenarios (Section 2.3) show that the average multiplicity in full phase space can be measured with 0.2% error with 10^5 events.

The ratio $D/\langle n \rangle$, where D is the dispersion, is constant if KNO scaling holds. KNO scaling is an asymptotic prediction: data at ISR energies are compatible with an ‘early’ KNO scaling, but Sp \bar{p} S data clearly showed a violation. Purely statistical extrapolation based on the above mentioned scenarios shows that the variance D^2 can be measured with less than 1% error with 10^5 events both in full phase space and within the ALICE acceptance.

3.2 Shape fits.

It will be possible to verify the extent of forward-backward (FB) correlations seen at Sp \bar{p} S and at Tevatron, to distinguish whether FB correlations grow or decrease and to study their link with the MD [17].

Predictions exist for the multiplicity distribution at 14 TeV, (e.g. [8, 9] and [18]; an alternative point of view on the two-component structure based on impact parameter analysis is presented in [19]). As previously explained in Section 2.3, in [8, 9] three scenarios can be distinguished at LHC by the value of $k^{-1} \approx D^2/\langle n \rangle^2$. It turns out that both in full phase space

and in restricted pseudo-rapidity regions the difference between the scenarios can be sharply defined if $D^2/\langle n \rangle^2$ is measured to 15% accuracy, as seen from the following table:

scenario	k^{-1}		
	f.p.s.	$ \eta < 1.5$	$ \eta < 1$
1	0.17	0.37	0.39
2	0.42	0.74	0.78
3	0.24	0.54	0.56

Purely statistical extrapolation shows that in these scenarios 10^5 events will yield 0.5% error, which is expected to be good enough to give extremely relevant information even if none of the envisaged scenarios turns out to be adequate (this would be a strong indication of the presence of an anomalous additional (hard?) component).

The scenarios and predictions should be confirmed not only by the analysis of the first two moments: the whole distribution should be involved. Purely statistical extrapolation shows that data produced in one scenario cannot be adequately fitted by either one of the other scenarios already with 10^5 events. Also fits based on one component only (of NB type) can be excluded with such statistics, as well as the other predictions.

Again on the global side, the information entropy $S = -\sum_n P_n \log P_n$ can be calculated and compared with the behaviour assumed in [20] and the one implicit in [8, 9]. Purely statistical extrapolations based on the latter reference show that information entropy can be measured to better than 0.1%, both in full phase space and in $|\eta| < 1$, with 10^5 events, which is more than enough to distinguish again the mentioned scenarios among them and from the expectation [20] of a scaling with available phase space. Incidentally, the latter option would produce a correction to $\langle n \rangle$ of a few percent, thus perfectly identifiable by LHC already with 10^5 events (ignoring again systematic errors).

Feynman scaling (dN/dy around $y = 0$ independent of \sqrt{s} , where y is the rapidity), introduced initially at ISR energies, has been shown to be violated at higher energies: as discussed previously in Section 2.3, the violation is due not only to the increasing importance of semi-hard events, but one expects a growth also of the semi-hard plateau; this should be checked at LHC.

The Ed^3N/dp^3 vs. p_t distribution is interesting because it can be compared with results from Tevatron and Sp̄pS. Is it possible to identify two (or more) components (e.g., different slopes) in this distribution, even if the soft events have a much smaller p_t than the hard ones? The CDF collaboration has shown that the single event's average p_t is a good candidate for event classification, especially in combination with the event multiplicity (see again Fig. 4). Multiplicity classes can be defined and whole distributions (e.g. in transverse momentum) can be looked at as a function of multiplicity or particle density [12]. Very interesting information for investigating the mechanism of particle production can come from the study of identified particles.

3.3 Sign oscillations of higher order moments.

H_q moments (the ratio of factorial, F_q , to cumulant, K_q , moments) are very important in defining substructures in the multiplicity distribution [21], as experimentally measured by L3 at LEP [22], but require very large statistics in order to be measured. Purely statistical extrapolations show that, in $|\eta| < 1$, 10^5 events allow to confidently calculate H_q up to order $q = 7$, but the expected 10^9 events, will allow to reach at least order $q = 14$, quite adequate for the purpose.

In fact H_q vs. q oscillations in hadron-hadron collisions in the GeV region [21, 8] and in e^+e^- annihilation at LEP energies [22] have been explained as the effect of the weighted superposition of classes of different topology, each class being described by a NBMD with different parameters. Observed shoulder structure in final charged particle multiplicity distributions and H_q vs. q oscillations have in this framework the same origin. In addition being H_q the ratio of factorial to cumulant moments, F_q/K_q , the occurrence of the NBMD for a sound description of H_q behaviour in each substructure via generalised local parton-hadron duality (GLPHD), i.e. the statement that F_q at hadron level is equal to $\rho^q F_q$ at parton level, with ρ defined by $\bar{n}_{\text{hadron}} = \rho \bar{n}_{\text{parton}}$, leads to the conclusion that H_q at hadron level coincide with H_q at parton level: an interesting possibility to understand deeply QCD and/or GLPHD.

3.4 Underlying event for Higgs production.

As Bjorken pointed out [23], at LHC energy processes will happen characterised by the presence of virtual electroweak bosons in the hard subprocess, like WW scattering via W or even Higgs exchange, with the bosons treated as partons of the proton beam. If the W 's then decay leptonically, a feature of the event will be a large rapidity gap, i.e., a region without hadrons separating the beam-jets containing the fragments of the projectiles. To turn this into a reliable signature, several issues were raised and discussed in [23]: one of them demands to know how big the rapidity gap must be in order that multiplicity fluctuations do not mimic the effect of W scattering and decay. To this question a detailed answer can be given by studying low multiplicity events: the scenarios previously described foresee 25 to 35% of events with less than 4 charged particles in the central region $|\eta| < 1.5$, which seems a considerable background to the W and Higgs events

One should also not forget that the ‘void probability’ P_0 , i.e., the probability of producing zero charged particles in a given rapidity interval, has interesting properties on its own, since in principle its \bar{n} dependence determines the full MD [24].

3.5 Quark-gluon plasma.

It has been argued that the increase of $\langle p_t \rangle$ from ISR to Sp \bar{p} S energies and its subsequent flattening with multiplicity could be an indication of a phase transition; this view has been abandoned and data analysed later in terms of phase space constraints and the emergence of mini-jets. CDF analysis (see Fig. 4) of $\langle p_t \rangle$ vs. central rapidity particle density, dN/dy , at 630 GeV and 1800 GeV reveals a different behaviour for soft and semi-hard events: a saturation is seen in soft events at $\langle p_t \rangle \approx 0.5$ GeV/ c , a fact to be contrasted with the increase from ≈ 0.44 up to ≈ 0.7 GeV/ c for (semi)hard events. In view of the high rapidity density expected with Alice, two important questions should be asked: *a)* does saturation effect for soft events continue up to 14 TeV, or, at a given particle rapidity density, $\langle p_t \rangle$ starts to increase again? In the latter case, could the sharp increase be indicative of a deconfinement transition in hot hadronic matter [25]? *b)* does $\langle p_t \rangle$ for semi-hard events continue to increase up to 14 TeV, or at a given particle rapidity density a saturation effect appears? One should expect that hard events at some particle rapidity density start to appear on top of the semi-hard ones in the first case, and the possible occurrence of a phase transition in the second one.

References

1. *Torino 2000: New Frontiers in Soft Physics and Correlations on the Threshold of the Third Millennium*, edited by A. Giovannini and R. Ugoccioni (Nucl. Phys. (Proc. Supp.) **B92** February, 2001).
2. T. Alexopoulos et al. (E735 Collaboration), Phys. Lett. **B435** (1998) 453.
3. G.J. Alner et al. (UA5 Collaboration), Physics Reports **154** (1987) 247.
4. R.E. Ansorge et al., (UA5 Collaboration), Z. Phys. **C43** (1989) 357.
5. G. Giacomelli and M. Jacob, Physics Reports **55** (1979) 1 .
6. C. Fuglesang, in *Multiparticle Dynamics: Festschrift for Léon Van Hove*, edited by A. Giovannini and W. Kittel (World Scientific, Singapore, 1990), p. 193.
7. C. Albajar et al. (UA1 Collaboration), Nucl. Phys. **B309** (1988) 405.
8. A. Giovannini and R. Ugoccioni, Phys. Rev. **D59** (1999) 094020.
9. A. Giovannini and R. Ugoccioni, Phys. Rev. **D60** (1999) 074027.
10. F. Abe et al. (CDF Collaboration), Phys. Rev. **D41** (1990) 2330.
11. D. Acosta et al., (CDF Collaboration), preprint FERMILAB-PUB-01/345-E, FERMI-LAB.
12. F. Rimondi, Nucl. Phys. (Proc. Suppl.) **B92** (2001) 114.
13. G. Bocquet et al. (UA1 Collaboration), Phys. Lett. **B366** (1996) 434.
14. B. Buschbeck and H.C. Eggers, Nucl. Phys. (Proc. Suppl.) **B92** (2001) 235; B. Buschbeck, H.C. Eggers and P. Lipa, Phys. Lett. **B481** (2000) 187.
15. Alexopoulos, T. et al. (E735 Collaboration), Phys. Rev. **D48** (1993) 984.
16. T. Alexopoulos et al., (E735 Collaboration), Phys. Rev. Lett. **64** (1990) 991.
17. G. Ekspong, in *XVI International Symposium on Multiparticle Dynamics*, edited by J. Grunhaus (Editions Frontières and World Scientific, Gif-sur-Yvette and Singapore, 1986), p. 309.
18. A. Kaidalov, talk at the Alice PPR meeting, CERN, April 2001.
19. J. Dias de Deus and R. Ugoccioni, Phys. Lett. **B469** (1999) 243.
20. V. Šimák, M. Šumbera and I. Zborovský, Phys. Lett. **B206** (1988) 159; M. Pachr, V. Šimák, M. Šumbera and I. Zborovský, Mod. Phys. Lett. **A77** (1992) 2333; M. Šumbera, talk at the Alice PPR meeting, CERN, April 2001.
21. A. Giovannini, S. Lupia and R. Ugoccioni, Phys. Lett. **B374** (1996) 231.
22. P. Achard et al, (L3 Collaboration), preprint CERN-EP/2001-072 (hep-ex/0110072), CERN.
23. J.D. Bjorken, Phys. Rev. **D47** (1993) 101.
24. S. Lupia, A. Giovannini and R. Ugoccioni, Z. Phys. **C66** (1995) 195.
25. L. Van Hove, Phys. Lett. **B118** (1982) 138.